Design of broadband beamformers robust against gain and phase errors in the microphone array characteristics — Source link ↗

Simon Doclo, Marc Moonen

Institutions: Katholieke Universiteit Leuven

Topics: Microphone array and Microphone

Related papers:

- Beamforming: a versatile approach to spatial filtering

- Practical supergain

- Superdirective Beamforming Robust Against Microphone Mismatch

- Robust adaptive beamforming

- Design of Robust Superdirective Arrays With a Tunable Tradeoff Between Directivity and Frequency-Invariance

DESIGN OF BROADBAND BEAMFORMERS ROBUST AGAINST MICROPHONE POSITION ERRORS

Simon Doclo, Marc Moonen

Katholieke Universiteit Leuven, Dept. of Elec. Engineering (ESAT - SISTA)
Kasteelpark Arenberg 10, 3001 Leuven, Belgium
{simon.doclo,marc.moonen}@esat.kuleuven.ac.be

ABSTRACT

Fixed broadband beamformers using small-sized microphone arrays are known to be highly sensitive to errors in the microphone array characteristics. This paper describes a procedure for designing broadband beamformers with an arbitrary spatial directivity pattern, which are robust against errors in the microphone positions. The presented design procedure optimises the mean performance of the broadband beamformer and hence requires knowledge of the probability density function of the microphone position errors. Simulations with a small-sized microphone array show the performance improvement that can be obtained by using a robust broadband beamformer design procedure.

1. INTRODUCTION

In many speech communication applications the microphone signals are corrupted by background noise and reverberation. Fixed and adaptive beamforming are well-known multi-microphone signal enhancement techniques for noise reduction and dereverberation [1]. Fixed beamformers are frequently used e.g. for creating the speech and the noise reference signals in a Generalised Sidelobe Canceller [2], for creating multiple beams, and in applications where the position of the desired speech source is approximately known, as in hearing aid and cochlear implant applications [3].

In [4][5] several procedures have been presented for designing broadband beamformers with an arbitrary spatial directivity pattern using an FIR filter-and-sum structure. Whatever design procedure is used, fixed beamformers are known to be highly sensitive to errors in the microphone array characteristics (gain, phase, position), especially when using small-sized arrays [6][7].

Robustness against random errors can be improved by limiting the white noise gain [6] or by performing a calibration procedure with the used microphone array [8]. However, when statistical knowledge about the errors is available, this knowledge can be incorporated into the design procedure. In [5][9] robust design procedures for (random) gain and phase errors have been presented. In this paper we extend one of these design procedures in order to include robustness against microphone position errors.

In Section 2 the far-field broadband beamforming problem is introduced. Section 3 discusses the weighted LS cost function, which can be used for broadband beamformer design when the microphone characteristics are exactly known. In Section 4 a robust beamformer design procedure is presented, which optimises the mean performance for (random) microphone position errors. In Section 5 simulation results are described and it is shown that robust broadband beamformer design gives rise to a significant performance improvement when microphone position errors occur.

2. BROADBAND BEAMFORMING: CONFIGURATION

Consider the linear microphone array depicted in Fig. 1, with N microphones, N L-taps FIR filters $\mathbf{w}_n$ (with real coefficients) and d_n the distance between the nth microphone and the centre of the microphone array. Assuming far-field conditions, the spatial directivity pattern $H(\omega, \theta)$ for a source $S(\omega)$ with normalised frequency ω at an angle θ from the microphone array is defined as

$$H(\omega, \theta) = \mathbf{w}^T \mathbf{g}(\omega, \theta) , \qquad (1)$$

with $\mathbf{w}$ the M-dimensional real-valued filter vector ($M = LN$), $\mathbf{w} = \begin{bmatrix} \mathbf{w}_0^T & \cdots & \mathbf{w}_{N-1}^T \end{bmatrix}^T$, and the steering vector $\mathbf{g}(\omega, \theta)$ equal to

$$\mathbf{g}(\omega, \theta) = \begin{bmatrix} \mathbf{e}^T(\omega)\, A_0(\omega, \theta)\, e^{-j\omega\tau_0(\theta)} \\ \vdots \\ \mathbf{e}^T(\omega)\, A_{N-1}(\omega, \theta)\, e^{-j\omega\tau_{N-1}(\theta)} \end{bmatrix} , \qquad (2)$$

with $\mathbf{e}(\omega) = \begin{bmatrix} 1 & e^{-j\omega} & \cdots & e^{-j(L-1)\omega} \end{bmatrix}^T$ and

$$A_n(\omega, \theta) = a_n(\omega, \theta)\, e^{-j\psi_n(\omega, \theta)}, \quad n = 0 \ldots N-1, \qquad (3)$$

representing the frequency and angle-dependent characteristics (gain, phase) of the nth microphone. The delay $\tau_n(\theta)$ is equal to

$$\tau_n(\theta) = \frac{d_n \cos\theta}{c} f_s , \qquad (4)$$

with c the speed of sound ($340\frac{m}{s}$) and f_s the sampling frequency.
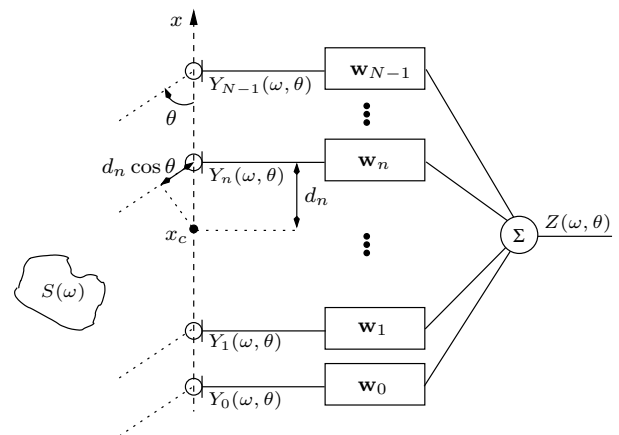

Fig. 1. Microphone array configuration (far-field assumption)

When a *microphone position error* occurs and the distance between the nth microphone and the centre of the array is $d_n + \delta_n$, this can be seen as a frequency and angle-dependent phase shift $\omega \frac{\delta_n \cos \theta}{c} f_s$ for the nth microphone, which hence can be easily incorporated into the microphone characteristics in (3) as

$$A_n(\omega, \theta) = \underbrace{a_n(\omega, \theta)}_{\text{gain}} \underbrace{e^{-j\psi_n(\omega, \theta)}}_{\text{phase}} \underbrace{e^{-j\omega \frac{\delta_n \cos \theta}{c} f_s}}_{\text{position}} . \quad (5)$$

Using (2), (4) and (5), the ith element of $\mathbf{g}(\omega, \theta)$ is equal to

$$\mathbf{g}^i(\omega, \theta) = e^{-j\omega \left(k + \frac{d_n \cos \theta}{c} f_s\right)} a_n(\omega, \theta) e^{-j\psi_n(\omega, \theta)} e^{-j\omega \frac{\delta_n \cos \theta}{c} f_s}, \quad (6)$$

with $k = \mathrm{mod}(i-1, L)$ and $n = \lfloor \frac{i-1}{L} \rfloor$. The steering vector $\mathbf{g}(\omega, \theta)$ can be decomposed into a real and an imaginary part, i.e. $\mathbf{g}(\omega, \theta) = \mathbf{g}_R(\omega, \theta) + j\mathbf{g}_I(\omega, \theta)$.

Using (1), the spatial directivity spectrum $|H(\omega, \theta)|^2$ is equal to

$$|H(\omega, \theta)|^2 = H(\omega, \theta)H^*(\omega, \theta) = \mathbf{w}^T \mathbf{G}(\omega, \theta)\mathbf{w} , \quad (7)$$

with $\mathbf{G}(\omega, \theta) = \mathbf{g}(\omega, \theta)\mathbf{g}^H(\omega, \theta)$. Using (6), the (i, j)-th element of $\mathbf{G}(\omega, \theta)$ is equal to

$$\mathbf{G}^{ij}(\omega, \theta) = e^{-j\omega \left((k-l) + \frac{(d_n - d_m)\cos \theta}{c} f_s\right)} a_n(\omega, \theta) a_m(\omega, \theta) \cdot$$
$$e^{-j\left(\psi_n(\omega, \theta) - \psi_n(\omega, \theta)\right)} e^{-j\omega \frac{(\delta_n - \delta_m)\cos \theta}{c} f_s} , \quad (8)$$

with $l = \mathrm{mod}(j-1, L)$ and $m = \lfloor \frac{j-1}{L} \rfloor$. The matrix $\mathbf{G}(\omega, \theta)$ can be decomposed into a real and an imaginary part $\mathbf{G}_R(\omega, \theta)$ and $\mathbf{G}_I(\omega, \theta)$. Since $\mathbf{G}_I(\omega, \theta)$ is anti-symmetric, $|H(\omega, \theta)|^2$ is equal to

$$|H(\omega, \theta)|^2 = \mathbf{w}^T \mathbf{G}_R(\omega, \theta)\mathbf{w} . \quad (9)$$

3. WEIGHTED LEAST-SQUARES COST FUNCTION

The design of a broadband beamformer consists of calculating the filter $\mathbf{w}$, such that $H(\omega, \theta)$ optimally fits the desired spatial directivity pattern $D(\omega, \theta)$, where $D(\omega, \theta)$ is an arbitrary 2-dimensional function. Several design procedures exist, depending on the specific cost function which is optimised. In this paper, we will only consider the weighted least-squares cost function. In [4][5][9], also eigenfilter-based and non-linear cost functions are discussed.

Considering the least-squares (LS) error $|H(\omega, \theta) - D(\omega, \theta)|^2$, the weighted LS cost function is defined as

$$J_{LS}(\mathbf{w}) = \int_\Theta \int_\Omega F(\omega, \theta)|H(\omega, \theta) - D(\omega, \theta)|^2 d\omega d\theta , \quad (10)$$

where $F(\omega, \theta)$ is a positive real weighting function, assigning more or less importance to certain frequencies and angles. This cost function can be written as the quadratic function

$$J_{LS}(\mathbf{w}) = \mathbf{w}^T \mathbf{Q}_{LS} \mathbf{w} - 2\mathbf{w}^T \mathbf{a} + d_{LS} , \quad (11)$$

with (assuming $D(\omega, \theta)$ to be real-valued)

$$\mathbf{Q}_{LS} = \int_\Theta \int_\Omega F(\omega, \theta) \, \mathbf{G}_R(\omega, \theta) \, d\omega d\theta \quad (12)$$

$$\mathbf{a} = \int_\Theta \int_\Omega F(\omega, \theta) D(\omega, \theta) \, \mathbf{g}_R(\omega, \theta) \, d\omega d\theta \quad (13)$$

$$d_{LS} = \int_\Theta \int_\Omega F(\omega, \theta) D^2(\omega, \theta) \, d\omega d\theta . \quad (14)$$

The filter $\mathbf{w}_{LS}$, minimising the weighted LS cost function, is

$$\mathbf{w}_{LS} = \mathbf{Q}_{LS}^{-1} \mathbf{a} . \quad (15)$$

4. ROBUSTNESS AGAINST POSITION ERRORS

Using the cost function in Section 3, it is possible to design beamformers when the microphone characteristics (gain, phase, position) are exactly known. However, small deviations from the assumed characteristics can lead to large deviations from the desired spatial directivity pattern [6][7]. Since in practice it is difficult to manufacture microphones with the same nominal gain and phase characteristics and microphone position errors frequently occur, a measurement or calibration procedure is required in order to obtain the true microphone characteristics. However, after calibration the microphone characteristics can still drift over time.

When statistical knowledge, e.g. a probability density function (pdf), is available for the gain, phase and position errors, this knowledge can be incorporated into a robust design procedure. In [5][9] two robust design procedures for frequency and angle-*in*dependent gain and phase errors have been presented. Considering all feasible characteristics, the first design procedure optimises the *mean performance*, i.e. the weighted sum of the cost functions, using the probability of the microphone characteristics as weights, whereas the second design procedure optimises the *worst-case performance*, i.e. the maximum cost function.

In this paper we extend the mean performance design procedure in order to include robustness against (random) microphone position errors. The mean performance weighted LS cost function can be written as

$$J_{LS}^m(\mathbf{w}) = \int_{A_0} \ldots \int_{A_{N-1}} J_{LS}(\mathbf{w}, \mathbf{A}) \, f_\mathcal{A}(A_0) \ldots f_\mathcal{A}(A_{N-1})$$
$$dA_0 \ldots dA_{N-1} , \quad (16)$$

with $J_{LS}(\mathbf{w}, \mathbf{A})$ the weighted LS cost function (11) for a specific microphone characteristic $\{A_0, \ldots, A_{N-1}\}$ and $f_\mathcal{A}(A)$ the joint pdf of the stochastic variables a (gain), ψ (phase) and δ (position error). Without loss of generality, we assume that *all microphone characteristics $A_n, n = 0 \ldots N-1$, are described by the same pdf $f_\mathcal{A}(A)$* and that a, ψ and δ are *independent stochastic variables*, such that the joint pdf is separable, i.e. $f_\mathcal{A}(A) = f_\alpha(a) f_\Psi(\psi) f_\Delta(\delta)$, with $f_\alpha(a)$ the gain pdf, $f_\Psi(\psi)$ the phase pdf and $f_\Delta(\delta)$ the position error pdf. These pdfs are normalised such that the area under the pdfs is equal to 1. By combining (11) and (16), the mean performance cost function can be written as

$$J_{LS}^m(\mathbf{w}) = \mathbf{w}^T \mathbf{Q}_m \mathbf{w} - 2\mathbf{w}^T \mathbf{a}_m + d_{LS} , \quad (17)$$

which has the same form as (11), with

$$\mathbf{a}_m = \int_{A_0} \ldots \int_{A_{N-1}} \mathbf{a} \, f_\mathcal{A}(A_0) \ldots f_\mathcal{A}(A_{N-1}) \, dA_0 \ldots dA_{N-1}$$

$$\mathbf{Q}_m = \int_{A_0} \ldots \int_{A_{N-1}} \mathbf{Q}_{LS} \, f_\mathcal{A}(A_0) \ldots f_\mathcal{A}(A_{N-1}) \, dA_0 \ldots dA_{N-1}.$$

We will now discuss the calculation of these two expressions.

4.1. Vector $\mathbf{a}_m$

Using (13), the vector $\mathbf{a}_m$ can be written as

$$\mathbf{a}_m = \int_\Theta \int_\Omega F(\omega, \theta) D(\omega, \theta) \, \mathbf{g}_{m,R}(\omega, \theta) \, d\omega d\theta , \quad (18)$$

with the (complex) vector $\mathbf{g}_m(\omega, \theta)$ equal to

$$\int_{A_0} \ldots \int_{A_{N-1}} \mathbf{g}(\omega, \theta) \, f_\mathcal{A}(A_0) \ldots f_\mathcal{A}(A_{N-1}) \, dA_0 \ldots dA_{N-1}. \quad (19)$$

$$\mathbf{g}_m^i(\omega,\theta) = e^{-j\omega\left(k+\frac{d_n\cos\theta}{c}f_s\right)} \underbrace{\int_{a_n} a_n(\omega,\theta)f_\alpha(a_n)\,da_n}_{\mu_a(\omega,\theta)} \underbrace{\int_{\psi_n} e^{-j\psi_n(\omega,\theta)}f_\Psi(\psi_n)\,d\psi_n}_{\mu_\psi(\omega,\theta)=\mu_{\psi,R}(\omega,\theta)+j\mu_{\psi,I}(\omega,\theta)} \underbrace{\int_{\delta_n} e^{-j\omega\frac{\delta_n\cos\theta}{c}f_s}f_\Delta(\delta_n)\,d\delta_n}_{\mu_\delta(\omega,\theta)=\mu_{\delta,R}(\omega,\theta)+j\mu_{\delta,I}(\omega,\theta)} \quad (20)$$

$$\mathbf{G}_m^{ij}(\omega,\theta) = e^{-j\omega\left((k-l)+\frac{(d_n-d_m)\cos\theta}{c}f_s\right)}\int_{a_n}\int_{a_m} a_n(\omega,\theta)\,a_m(\omega,\theta)f_\alpha(a_n)f_\alpha(a_m)\,da_n da_m \;\cdot \quad (21)$$

$$\int_{\psi_n}\int_{\psi_m} e^{-j\left(\psi_n(\omega,\theta)-\psi_m(\omega,\theta)\right)}f_\Psi(\psi_n)f_\Psi(\psi_m)\,d\psi_n d\psi_m \int_{\delta_n}\int_{\delta_m} e^{-j\omega\frac{(\delta_n-\delta_m)\cos\theta}{c}f_s}f_\Delta(\delta_n)f_\Delta(\delta_m)\,d\delta_n d\delta_m$$

Using (6), the ith element of $\mathbf{g}_m(\omega,\theta)$ is equal to (20), with $\mu_a(\omega,\theta)$ real-valued and $\mu_\psi(\omega,\theta)$ and $\mu_\delta(\omega,\theta)$ complex-valued (for symmetric pdfs around 0, $\mu_\psi(\omega,\theta)$ and $\mu_\delta(\omega,\theta)$ are also real-valued). In the remainder of this paper we will assume Gaussian pdfs, e.g. the microphone position error pdf $f_\Delta(\delta)$ is assumed to be

$$f_\Delta(\delta) = \frac{1}{\sqrt{2\pi s_\delta^2}}e^{-\frac{(\delta-u_\delta)^2}{2s_\delta^2}} , \quad (22)$$

with mean u_δ and variance s_δ. Using (22) and the fact that

$$\int_{-\infty}^{\infty} e^{-jbx}e^{-ax^2}\,dx = \sqrt{\frac{\pi}{a}}e^{-\frac{b^2}{4a}} , \quad (23)$$

it can be easily shown that

$$\mu_\delta(\omega,\theta) = e^{-\frac{(\omega s_\delta\cos\theta f_s)^2}{2c^2}}e^{-j\omega\frac{u_\delta\cos\theta}{c}f_s} , \quad (24)$$

such that the ith element of the real part $\mathbf{g}_{m,R}(\omega,\theta)$ is equal to

$$\mu_a(\omega,\theta)\left\{\mu_{\psi,R}(\omega,\theta)\cos\left[\omega\left(k+\frac{(d_n+u_\delta)\cos\theta}{c}f_s\right)\right]+\right. \quad (25)$$

$$\left.\mu_{\psi,I}(\omega,\theta)\sin\left[\omega\left(k+\frac{(d_n+u_\delta)\cos\theta}{c}f_s\right)\right]\right\}e^{-\frac{(\omega s_\delta\cos\theta f_s)^2}{2c^2}}.$$

A similar expression can be obtained for a uniform pdf. Using (25), the ith element of $\mathbf{a}_m$ in (18) can be calculated by (numerically) integrating the expression $F(\omega,\theta)D(\omega,\theta)\mathbf{g}_{m,R}^i(\omega,\theta)$ over the considered frequency-angle region.

4.2. Matrix $\mathbf{Q}_m$

Using (12), the matrix $\mathbf{Q}_m$ can be written as

$$\mathbf{Q}_m = \int_\Theta\int_\Omega F(\omega,\theta)\,\mathbf{G}_{m,R}(\omega,\theta)\,d\omega d\theta , \quad (26)$$

with the (complex) matrix $\mathbf{G}_m(\omega,\theta)$ equal to

$$\int_{A_0}\cdots\int_{A_{N-1}}\mathbf{G}(\omega,\theta)\,f_\mathcal{A}(A_0)\ldots f_\mathcal{A}(A_{N-1})\,dA_0\ldots dA_{N-1}. \quad (27)$$

Using (8), the (i,j)-th element of $\mathbf{G}_m(\omega,\theta)$ is equal to (21). If $n=m$, the (i,j)-th element of the real part $\mathbf{G}_{m,R}(\omega,\theta)$ is equal to

$$\mathbf{G}_{m,R}^{ij}(\omega,\theta) = \sigma_a^2(\omega,\theta)\,\cos\left[\omega(k-l)\right] , \quad (28)$$

with

$$\sigma_a^2(\omega,\theta) = \int_a a^2(\omega,\theta)f_\alpha(a)\,da . \quad (29)$$

If $n\neq m$, the (i,j)-th element of the real part $\mathbf{G}_{m,R}(\omega,\theta)$ is equal to

$$\mu_a^2(\omega,\theta)\sigma_\psi^2(\omega,\theta)\sigma_\delta^2(\omega,\theta)\cos\left[\omega\left((k-l)+\frac{(d_n-d_m)\cos\theta}{c}f_s\right)\right] , \quad (30)$$

with $\sigma_\psi^2(\omega,\theta)$ equal to

$$\int_{\psi_1}\int_{\psi_2} e^{-j\left(\psi_1(\omega,\theta)-\psi_2(\omega,\theta)\right)}f_\Psi(\psi_1)f_\Psi(\psi_2)\,d\psi_1 d\psi_2 ,$$

and $\sigma_\delta^2(\omega,\theta)$ similarly defined. In [9] it has been shown that

$$\sigma_\psi^2(\omega,\theta) = \mu_{\psi,R}^2(\omega,\theta)+\mu_{\psi,I}^2(\omega,\theta) , \quad (31)$$

such that using the same arguments and using (24), it can be easily proved that

$$\sigma_\delta^2(\omega,\theta) = \mu_{\delta,R}^2(\omega,\theta)+\mu_{\delta,I}^2(\omega,\theta) = e^{-\frac{(\omega s_\delta\cos\theta f_s)^2}{c^2}} . \quad (32)$$

Using (28) and (30), the (i,j)-th element of $\mathbf{Q}_m$ in (26) can be calculated by integrating the expression $F(\omega,\theta)\mathbf{G}_{m,R}^{ij}(\omega,\theta)$ over the considered frequency-angle region.

5. SIMULATIONS

We have performed simulations using a small-sized non-uniform linear microphone array consisting of $N=3$ microphones at positions $\begin{bmatrix}-0.01 & 0 & 0.015\end{bmatrix}$ m. We have designed an end-fire broadband beamformer with passband specifications $(\Omega_p,\Theta_p) = (300\text{–}4000\,\text{Hz}, 0°\text{–}60°)$ and stopband specifications $(\Omega_s,\Theta_s) = (300\text{–}4000\,\text{Hz}, 80°\text{–}180°)$ and $f_s = 8\,\text{kHz}$. The filter length $L=20$ and the weighting function $F(\omega,\theta)=1$.

In order to only investigate the effect of microphone position errors, the microphones are assumed to be omni-directional microphones with a frequency response equal to 1, i.e. $a_n(\omega,\theta)=1$ and $\psi_n(\omega,\theta)=0$, $n=0\ldots N-1$, simplifying several expressions ($\mu_a(\omega,\theta)=\mu_\psi(\omega,\theta)=\sigma_a^2(\omega,\theta)=\sigma_\psi^2(\omega,\theta)=1$). We have designed 3 types of broadband beamformers:

1. a non-robust beamformer, i.e. assuming no microphone position errors ($\delta_n=0$, $n=0\ldots N-1$)

2. a robust beamformer (**MIC**) using a Gaussian microphone position error pdf with $u_\delta=0$ and $s_\delta=0.003$ (these values depend on the accuracy of the manufacturing process of the microphone arrays)

3. since a microphone position error δ corresponds to a maximum phase error $\psi_{max}=\pi\frac{\delta}{c}f_s$ (at $\omega=\pi$ and $\theta=0°$), we have designed several robust beamformers (**CPH**) assuming a constant (frequency and angle-independent) phase error, i.e.

$$\mu_\delta(\omega,\theta) = e^{-\frac{s_\psi^2}{2}} = e^{-\frac{(\pi s_\delta f_s)^2}{2c^2}} , \quad \sigma_\delta^2(\omega,\theta) = e^{-s_\psi^2} .$$

The microphone position error $s_\delta=0.003\,\text{m}$ corresponds to the phase error $s_\psi=12.7°$.

For the different design procedures, Fig. 2 plots the mean performance weighted LS cost function $J_{LS}^m(\mathbf{w})$ for the Gaussian microphone position error pdf. Obviously, the MIC-robust beamformer gives rise to the smallest cost function, whereas the non-robust

beamformer gives rise to the largest cost function. The CPH-robust beamformers are less robust than the MIC-robust beamformer, but even for small values of s_ψ they still provide a substantial robustness increase compared to the non-robust beamformer.

Figures 3 and 4 show the spatial directivity plots at several frequencies for the non-robust beamformer and for the MIC-robust beamformer, both when no errors occur and when (small) microphone position errors $\begin{bmatrix} 0.002 & -0.002 & 0.002 \end{bmatrix}$ m occur. When no errors occur, the performance of the non-robust beamformer is the best, but the performance of the MIC-robust beamformer is certainly acceptable. However, when microphone position errors occur, the performance of the non-robust beamformer deteriorates considerably, certainly at low frequencies. On the other hand, the MIC-robust beamformer retains the desired spatial directivity pattern, even when microphone position errors occur.

6. CONCLUSION

In this paper, a procedure has been described for designing broadband beamformers that are robust against random microphone position errors. This design procedure optimises the mean performance, requiring knowledge about the microphone position error pdf, and is in fact an extension of a robust design procedure presented in [9]. Specific expressions have been derived for a Gaussian pdf. Simulations have illustrated the performance improvement that is obtained when microphone position errors occur.

7. REFERENCES

[1] B. D. Van Veen and K. M. Buckley, "Beamforming: A Versatile Approach to Spatial Filtering," *IEEE ASSP Magazine*, vol. 5, no. 2, pp. 4–24, Apr. 1988.

[2] S. Nordebo, I. Claesson, and S. Nordholm, "Adaptive beamforming: Spatial filter designed blocking matrix," *IEEE Journal of Oceanic Engineering*, vol. 19, no. 4, pp. 583–590, Oct. 1994.

[3] R. W. Stadler and W. M. Rabinowitz, "On the potential of fixed arrays for hearing aids," *Journal of the Acoustical Society of America*, vol. 94, no. 3, pp. 1332–1342, Sep. 1993.

[4] S. Doclo and M. Moonen, "Design of far-field broadband beamformers using eigenfilters," in *Proc. European Signal Proc. Conf.*, Toulouse, France, Sep. 2002, pp. III 237–240.

[5] S. Doclo, *Multi-microphone noise reduction and dereverberation techniques for speech applications*, Ph.D. thesis, ESAT, Katholieke Universiteit Leuven, Belgium, May 2003.

[6] H. Cox, R. Zeskind, and T. Kooij, "Practical supergain," *IEEE Trans. Acoust., Speech, Signal Processing*, vol. 34, no. 3, pp. 393–398, June 1986.

[7] M. Buck, "Aspects of first-order differential microphone arrays in the presence of sensor imperfections," *European Trans. on Telecommunications*, vol. 13, no. 2, pp. 115–122, Mar-Apr 2002.

[8] C. Sydow, "Broadband beamforming for a microphone array," *Journal of the Acoustical Society of America*, vol. 96, no. 2, pp. 845–849, Aug. 1994.

[9] S. Doclo and M. Moonen, "Design of robust broadband beamformers for gain and phase errors in the microphone array characteristics," *Accepted for publication in IEEE Trans. Signal Processing*, 2003. Available at ftp://ftp.esat.kuleuven.ac.be/pub/SISTA/doclo/reports/02-111.ps.gz
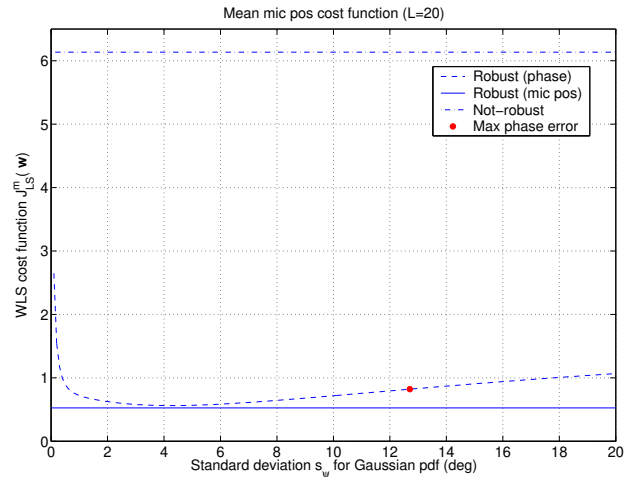
Fig. 2. Mean performance weighted LS cost function $J_{LS}^m(\mathbf{w})$ for non-robust and robust design procedures (MIC, CPH)
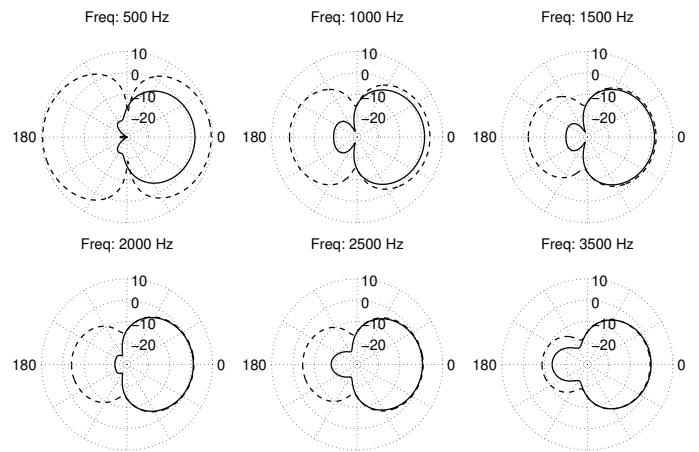

Fig. 3. Spatial directivity plots for non-robust beamformer (no errors: solid line, microphone position errors: dashed line)
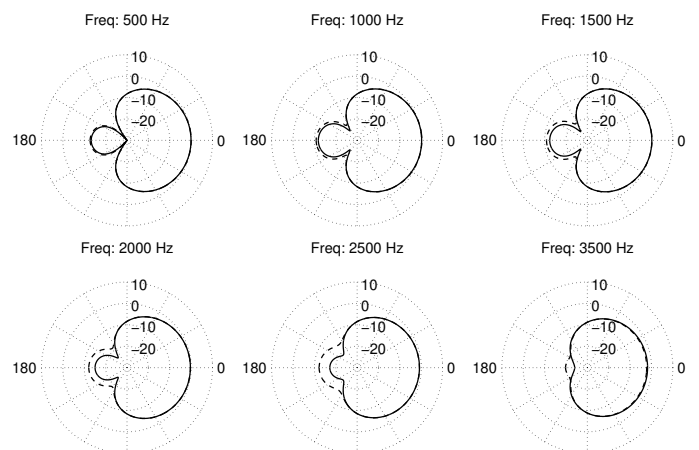

Fig. 4. Spatial directivity plots for MIC-robust beamformer (no errors: solid line, microphone position errors: dashed line)